STUDY OF AN OBSERVED LOW-LEVEL JET THROUGH LARGE-EDDY SIMULATIONS

J. Cuxart * and M.A. Jiménez

Universitat de les Illes Balears, Spain

1 INTRODUCTION

The Stable Atmospheric Boundary Layer Experiment in Spain-1998 (SABLES-98, Cuxart et al., 2000a) took place during 14 days in September 1998 at the CIBA site on the Northern Spanish Plateau. This is the upper part of the Duero River Basin, an elevated flat area with a radius of about 150 km and a height of about 800 m above sealevel (ASL) surrounded by mountain ranges with peaks up to 2500 m ASL. Nevertheless the basin has a slight slope of about 300 m from the northern and southern parts to the central area, where the Duero river flows from east to west. A 100 m tower was setup, with sonic anemometers mounted at 6, 13 and 32 m above the ground-level (AGL) and captive balloons were released continuously.

In most of the more stable nights, Low-Level Jets (LLJs) were observed and their main features are analyzed in Conangla and Cuxart (2006, from now on CC2006). Basically, they consisted of a flow from the East, with maximum wind speed around 8-9 m s^{-1} located somewhere between 60 and 100 m AGL.

In CC2006, one of the observed LLJ was chosen for a more detailed study using a single-column model (described in Cuxart et al., 2000b). The main purpose was to see if the model was able to generate turbulent motions at the upper part of the LLJ (above the maximum wind speed) as the low-values of the Richardson number computed from the soundings seemed to indicate. The model showed that conditions are met for turbulence mixing in that layer, basically due to shear production combined with a weak temperature gradient. An elevated layer of turbulence at a height between 1 and 3 times the height of the wind maximum (h_{LLJ}) was found, similarly to what Smedman et

al. (1993) had previously indicated for a marine LLJ. Both turbulent layers were practically decoupled, as seen in the turbulence kinetic energy (TKE) budget, where near h_{LLJ} there is a layer with almost no TKE.

Here a similar approach will be followed, but using now a Large-Eddy Simulation (LES) as the analyzing tool. The main interest is to describe how the turbulence mixing takes place below, across and above the level of the wind maximum, usually coincident with a temperature inversion. Further details are found in Cuxart and Jiménez (2006). Although the LES of the stably stratified atmospheric boundary layer (SBL) is difficult, due to the fact that stability of stratification introduces anisotropy and the vertical dimension of the eddies can be very small, Jiménez and Cuxart (2005) showed that, for this particular LES model, the main features of the SBL are well reproduced when compared to observational data.

2 MODELLING CONFIGURATION AND STRATEGY

A simulation of a stationary LLJ observed in SABLES-98 from midnight to 0200 UTC of the 21st September is made. The Meso-NH model (Lafore et al., 1998) is run in LES configuration (Cuxart et al. 2000b), taking a domain size of 600×400×800 m, using 100×100×150 grid points in the x, y, and z directions, respectively. The horizontal grid spacing is 6 m for x and 4 m for y. The vertical grid spacing changes with height; the vertical resolution is larger near the ground, constant (2 m) until 100 m, stretched until 400 m where it is about 5 m, and stretched further until 800m, where it is about 30 m.

The latitude (43°) and the roughness length (z_0=0.035 m) correspond to the SABLES-98 site (Cuxart et al., 2000a). Since the observed LLJ is quasi-stationary between 0030 UTC and 0200 UTC, the initial temperature and wind profiles

---
*Corresponding author address: Joan Cuxart, Dpt. Fisica, Universitat de les Illes Balears, Carret. Valldemossa, km 7.5, 07122-Palma de Mallorca, Spain; email:joan.cuxart@uib.es
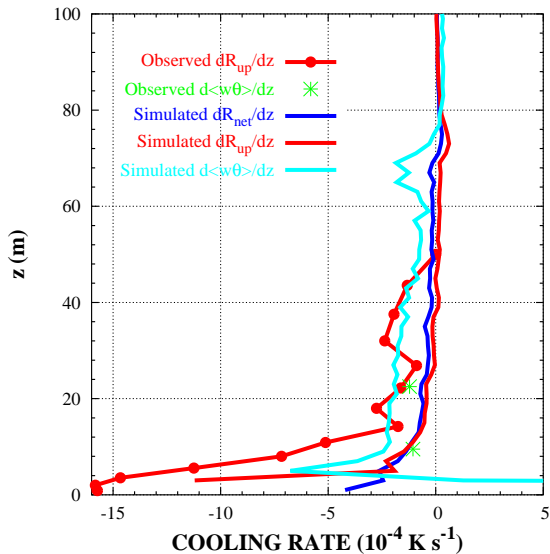
Figure 1: Radiative and turbulent coolings computed from the LES (in lines) and estimated from the data using the temperature measured in the tower (lines and points) between 00UTC and 02UTC

for the LES model are taken from the 0030 UTC sounding (see Figures 2.a and 2.b) within this period. The measured relative humidity during that night was below 50% and therefore, effects of moisture are not considered in this study, at the risk of underestimating the effect of the radiation.

As in CC2006, the geostrophic wind is prescribed constant in time, with a value of 6 m s^{-1} below the maximum of the wind and a linear decrease above it up to 350 m, from where its value is 2 m s^{-1} until the top of the domain. This variation with height is necessary to maintain the jet during the simulation, as it happens for CC2006. The amount of change is not critical, although it is chosen to be consistent with the thermal wind associated with the climatologically observed temperature difference across the northern Duero basin. A small random perturbation is added to all velocity components to initiate the resolved motions.

The radiation scheme of Morcrette (1990) is used since its contribution is extremely important for the near-the-surface cooling under clear-sky nights with weak winds, as Garratt and Brost (1982) or André and Mahrt (1982) showed. Above the surface layer, the radiative cooling becomes fairly independent of the height above the ground and it is only about a 20% of the turbulence con-

tribution (Tjemkes and Duynkerke, 1989). This is the behavior found in the present simulation, as shown in Figure 1, where the modelled contributions are compared to estimations from the observations of the studied night.

To allow feedbacks between the soil and the atmosphere, a very simple energy balance equation (Van de Wiel et al., 2002) has been considered, where the three terms that balance are the turbulent heat flux, the flux from the soil and the longwave radiative flux. This method has already been tested in Jiménez and Cuxart (2005) keeping the same values for the physiographical parameters. From this energy balance equation, the averaged surface vertical flux converges to about -0.012 K m s^{-1} at 2 m, larger than the one measured during the stationary period (-0.005 K m s^{-1}) at 6 m; this stronger cooling flux sustained during four hours leads to a smaller surface temperature than the observed one at the end of the run. The simulated conditions converge to a surface flux of -0.012 K m s^{-1} and they are well within the range of observable conditions following Derbyshire (1990), where the maximum value for the surface flux is -0.015 K m s^{-1}, assuming a critical Richardson number of 0.25.

The run lasts 4 h and horizontal half-hourly averages are taken.

3 DESCRIPTION OF THE MEAN STATE AND THE TURBULENCE STATISTICS

The observed wind speed and potential temperature profiles taken from the soundings and the ones obtained from the LES are shown in Figure 2. The simulation is able to reproduce many of the relevant features, such as the height and intensity of the jet and the shear from the maximum wind speed or "nose" to the ground. However, the simulation shows a monotonic increase of the height of the nose from 65 to 71 m, unlike the observed evolution. Above the nose, the simulated wind experiences a rotation similar to the inertial oscillation, although slightly slowed down by the weak turbulence mixing above the jet. The soundings do not rotate in the same way, indicating that the setup misses some external forcing or a stronger elevated turbulence.

The potential temperature provided by the simulation compares fine to the observations above the nose, but tends to diverge from them below.
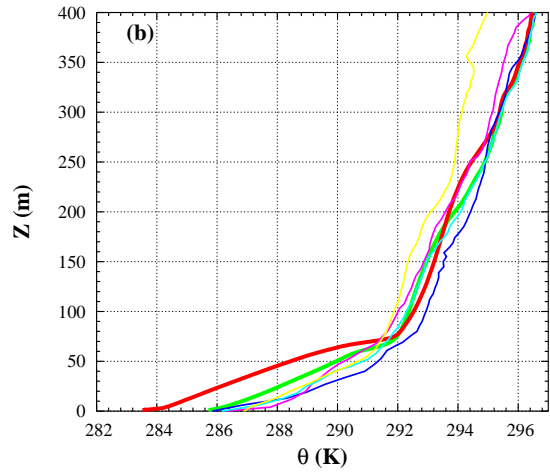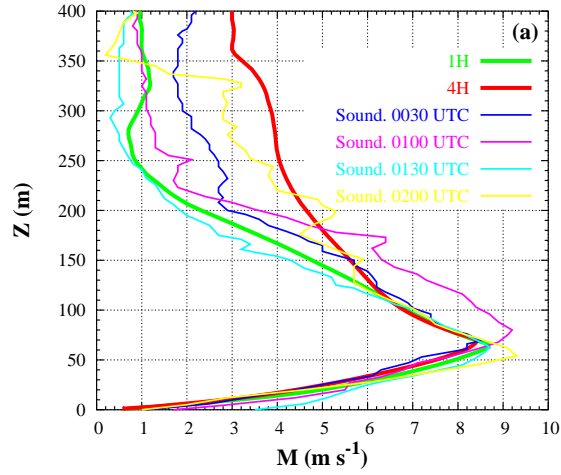
Figure 2: Half-hourly averaged LES outputs at 1h (thick green line) and 4h (thick red line) and some soundings (thin lines) for (a) wind speed and (b) potential temperature
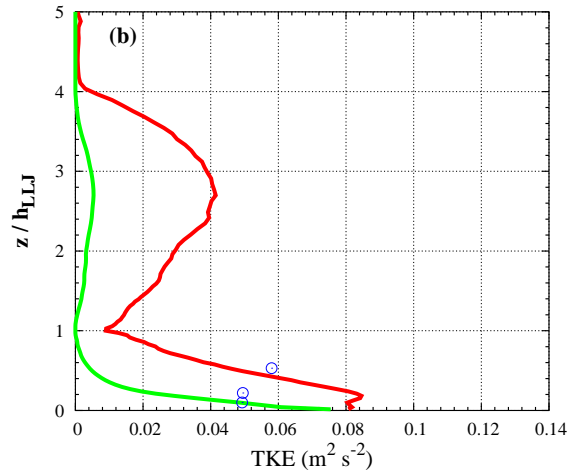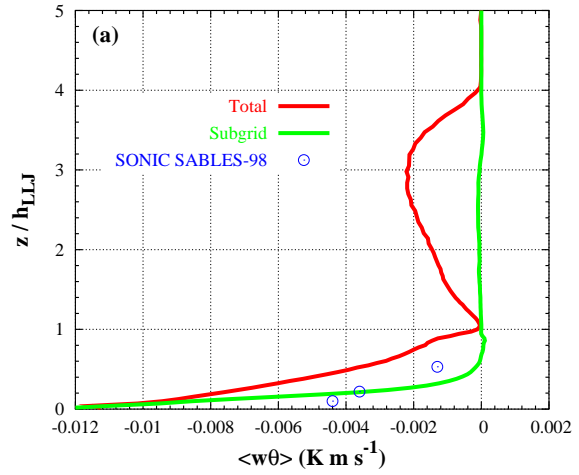

Figure 3: Averaged LES outputs at 4h: total and subgrid (a) heat flux and (b) Turbulence Kinetic Energy. Symbols are averages from sonic anemometers. The y-axis is normalized by the LLJ height (h_{LLJ})

The simulation misses completely the very strongly stratified layer near the ground and cools all the layer below the nose, allowing the shear to generate more turbulence that can reach the ground. This effect cumulates during all the simulation resulting in a final profile 2 K too low in the surface layer. Sensitivity tests on this point have been performed but none manages to correct this default.

Some turbulence moments are shown in Figure 3. They all share a two-layered structure with minimum intensity at the nose. At the inversion, the heat flux (both resolved and subgrid) is very close to zero, indicating that, in average, there is a very small transport of heat between the layers as seen in the 30-minute averages. This does not exclude, as we will see later, that the mixing can take place in short episodes, wiped away by the averaging procedure. The comparison to fluxes computed from the sonics indicates that the model tends to overestimate the flux in the lower layer, but nothing can be said of what happens at the level of the inversion and above.

The TKE shows significant values at the inversion level, all resolved and mostly (but not all) attributable to the resolved horizontal variances (not shown). The values below the nose are well captured although the slight increase with height is missing. Above the nose, the TKE is of the same order of magnitude as below, with a maximum at near 3 times the height of the nose, consistently with the observations of Smedman et al. (1993) for a jet over the Baltic Sea or in CC2006 for this same site.

4   MIXING ACROSS THE WIND MAXIMUM

Figures 2 and 3 show that the model is not capturing the main features of the surface, where large gradients of temperature exist in the first meters. Apparently, with the resolution used, the model is not able to stay at almost constant values of the 2 m temperature as observed, maybe because this feature might be due to an external forcing ignored in the simulation setup, such as a very thin drainage flow. In order to see if such a behavior could be imposed in the simulation, the same balance equation is run using the wind and temperature at the first level of the model prescribed and constant, and equal to the observed average values (1.4 m s^{-1} and 286 K).

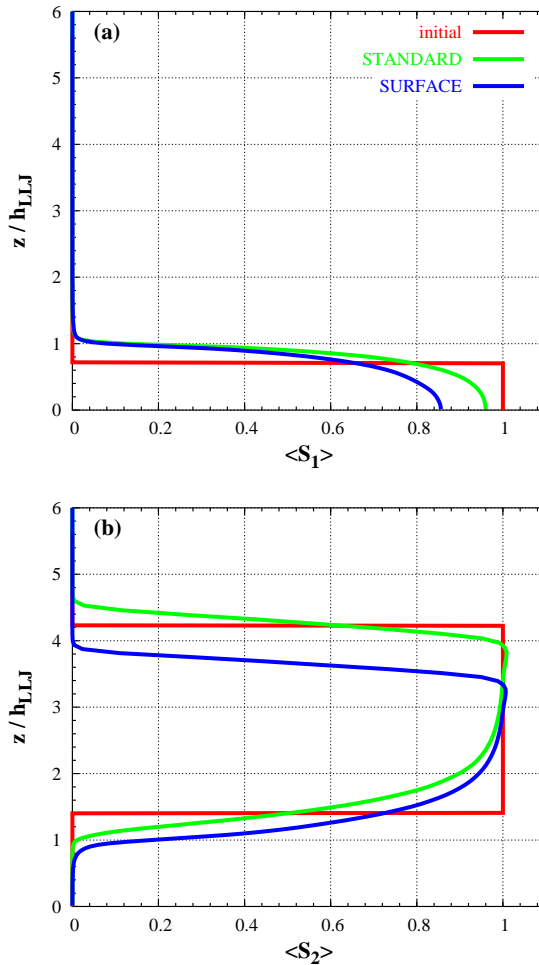One hour after the start, two scalars are in-

Figure 4: Averaged scalar concentrations of (a) S_1 and (b) S_2 after 4h from the beginning of the run. The y-axis is normalized by the LLJ height (h_{LLJ}) obtained for each case
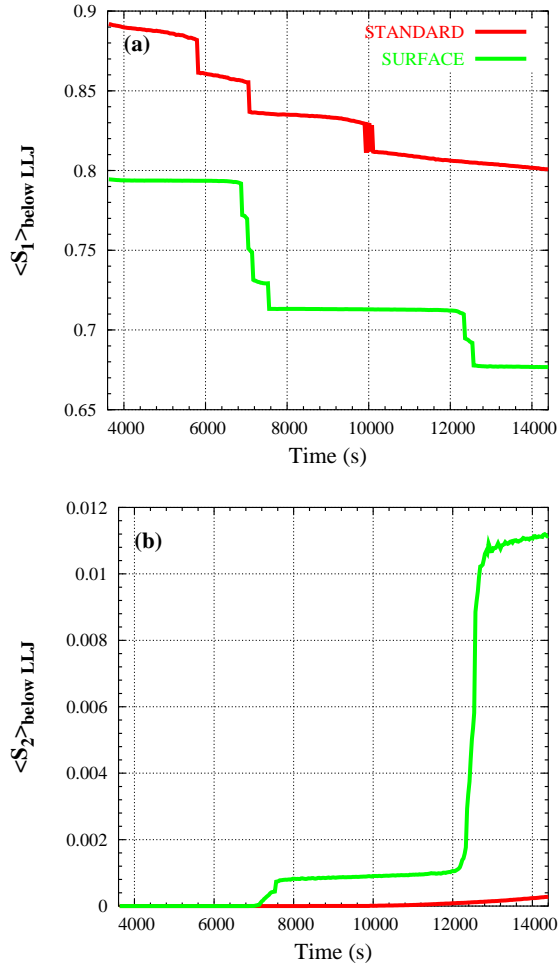
Figure 5: Time series of the averaged scalar from the ground up to the LLJ height (h_{LLJ}): (a) S_1 and (b) S_2

troduced, one below (S_1) and one above (S_2) the wind maximum (see Figure 4). They are used to inspect the mixing above, below and across the LLJ maximum, as in Wyngaard and Brost (1984) top-down and bottom-up transport in a convective boundary layer. Both scalars are immediately well mixed within their layer and reach the inversion. After four hours of simulation, a small amount of scalar has crossed the inversion in both senses, and there is no numerical loss of scalar in the process. It is clear in Figure 4.a that more scalar is transported across the inversion upwards when the model is forced with observed surface layer conditions. Since this simulation experiences intermittent turbulence, it seems that this procedure is more efficient in transporting mass across the jet that the diffusive-like mixing across the inversion produced by the standard simulation.

Some more insight can be gained inspecting the temporal evolution of the layer-averaged amounts of scalar. Regarding the transport from below to above the jet (Figure 5.a), the standard simulation has very weak continuous mixing with several bursts not evenly distributed. The forced simulation does not mix continuously across the inversion, but is very efficient in mixing in the oddly distributed turbulent bursts across the jet. The mixing from above to the subjet layer (Figure 5.b), shows that it is less efficient than in the other sense, but that it is clearly enhanced in the case of the surface-forced simulation, especially during the turbulence bursts.

5   COMPARISON OF OBSERVED AND SIMULATED PDFs

Although there were only sonic anemometer measurements up to 32 m, there were more conventional sensors recording at a rate of 5 Hz, up to 50 m for the temperature and up to 100 m for the wind. In order to see up to what point the LES simulation is realistic beyond the comparison of averaged values, we inspect here the Probability Density Functions (PDFs) measured by those sensors and those produced by the LES at the same levels, the latter computed taking a complete horizontal field every minute during the last hour of the simulation.

The PDFs for any variable x (B(x)) are normalized such that $\int_{-\infty}^{\infty} B(x)dx = 1$, and, to allow for a clear comparison to other series, they are customarily plotted using $\sigma_x B(x')$ where $x' = \frac{x - \overline{x}}{\sigma_x}$.
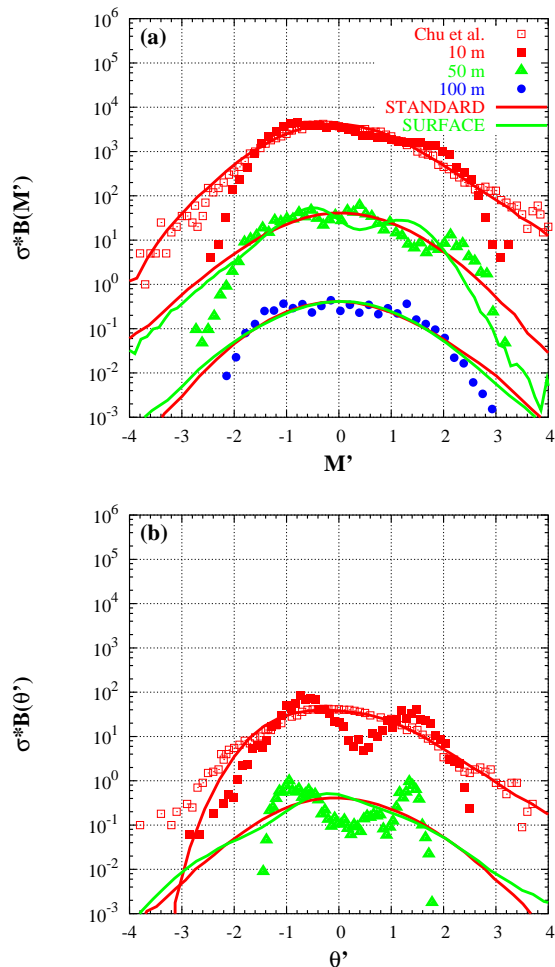
5

Figure 6: Normalized PDFs for (a) wind speed and (b) potential temperature computed from data (points) and from the LES (lines) at 10 m, 50 m and 100 m. The PDFs at 50 m and 100 m have been shifted up two and four decades respectively to clarify the intercomparison. In open squares, PDFs obtained from data measurements in Chu et al. (1996)

Here, $\overline{x}$ is the mean value and σ_x the standard deviation; a logscale is chosen for the y-axis to better inspect the tails (Figure 6). Further explanations are given in Jiménez and Cuxart (2006).

Figure 6.a compares the PDFs for the fluctuations of the wind speed at 3 levels and also to some measurements by Chu et al. (1996) in the stably stratified surface layer. Two different PDFs have been computed from the LES corresponding to the standard run and the one where the observed surface temperature and wind speed have been imposed. The LES model at 10 m fits better to Chu et al. data than to SABLES-98 data. This can be explained by the fact that Chu et al. measured in a classical surface-induced shear-driven SBL, well described by the similarity theory, which is imposed in the first level of the LES model. SABLES-98 data, with a LLJ, surely does not fit very well with the standard similarity theory, as the tails show. On the other hand, the PDF of the surface-forced LES has some fluctuations close to the mean value, in agreement with the observations. At 100 m, above the wind maximum, the simulations give very similar results and they compare fairly well to data, although some discrepancies still exist at the tails. This comparison gives support to the idea that the simulation is more realistic above than below the wind maximum.

The fluctuations of temperature at 10 and 50 m are compared in Figure 6.b. It is very worthy to note here that the observed data show a very clearly defined binormal distribution, both at 10 and at 50 m, with values as significant as ± 0.5 K. The observations could therefore indicate that the mixing below the LLJ maximum is performed either by large eddies, suddenly bringing warmer air to the surface that cools until a new event takes place, or that there could be intrusive bursts from above with a certain periodicity. The standard LES is clearly not able to produce this kind of distribution, and acts more as a system immediately reducing any too large gradient that is formed in the layer. The surface-forced LES introduces some asymmetry but is still far from the observations.

6 CONCLUSIONS

An LES simulation of a LLJ based on field observations has been performed. The model is able to reproduce the observed two-layered structure, consistent in two turbulent layers separated by a temperature inversion very close to the height of

the maximum wind speed. The upper layer characteristics are well captured quite independently on the conditions of the surface, but the results vary significantly in the subjet layer depending on the surface boundary conditions. The radiation is a feature that has to be included in such a study in order to capture adequately the temperature balance close to the surface. However, more resolution would be needed to properly represent the strong temperature gradient near-the ground.

The inversion at the jet acts as barrier to the turbulence transport across the layers, being even more stable than the surface layer. The two layers act almost independently but, depending on the configuration of the simulation, can exchange heat and matter, basically through short-lasting turbulence bursts. The modeled bursts are similar to some observed events. The challenge would be to measure effective transport across the jet and develop a parameterization of intermittent mixing for it.

References

André, J.C., and Mahrt, L. (1982). The nocturnal surface inversion and influence of clear-air radiative cooling. *J. Atmos. Sci.*, **39**, 864-878.

Chu, C.R., Parlange, M.B., Katul, G.G., and Albertson, J.D. (1996). Probability density functions of turbulent velocity and temperature in the atmospheric surface layer. *Water Resources Research* **32**, 1681–1688.

Conangla, L. and Cuxart, J. (2006). On the turbulence at the upper part of the LLJ: An experimental an numerical study. *Bound.-Layer Meteor., in press*

Cuxart, J. and Jiménez, M. A. (2006). Mixing processes in a nocturnal Low-Level Jet. *Submitted to J. Atmos. Sci.*

Cuxart, J., Yagüe, C., Morales, G., Terradellas, E., Orbe, J., Calvo, J., Fernandez, A., Soler, M. R., Infante, C., Buenestado, P., Espinalt, A., Joergensen, H. E., Rees, J. M., Vilá, J., Redondo, J. M., Cantalapiedra, I. R., and Conangla, L. (2000a). Stable Atmospheric Boundary-Layer Experiment in Spain (SABLES-98): A report. *Bound.-Layer Meteor.*, **96**, 337-370.

Cuxart, J., Bougeault, P. and Redelsperger, J.-L. (2000b). A turbulence scheme allowing for mesoscale and large-eddy simulations. *Q. J. R. Meteorol. Soc.*, **126**, 1–30.

Derbyshire, S. H. (1990). Nieuwstadt's stable boundary layer revisited. *Quart. J. Roy. Meteor. Soc.*, **116**, 127-158.

Garratt, J.R., and Brost, R.A. (1982). Radiative cooling effects within and above the nocturnal boundary layer. *J. Atmos. Sci.*, **38**, 2730-2746.

Jiménez, M. A., and Cuxart, J. (2005). Large-eddy Simulations of the Stable Boundary Layer using the standard Kolmogorov theory: range of applicability *Bound.-Layer Meteor.*, **115**, 241-261.

Jiménez, M. A., and Cuxart, J. (2006). Study of the probability density functions from a Large-eddy simulation of a stably stratified case. *Bound.-Layer Meteor., in press*

Lafore, J.P., Stein, J., Asencio, N., Bougeault, P., Ducrocq, V., Duron, J., Fisher, C., Héreil, P., Mascart, P., Masson, V., Pinty, J.P., Redelsperger, J.-L., Richard, E. and Vilà-Guerau de Arellano, J. (1998). The Meso-NH atmospheric simulation system. Part I: Adiabatic formulation and control simulation. *Ann. Geophys.*, **16**, 90-109.

Morcrette, J.-J. (1990). Impact of changes to the radiation transfer parameterizations plus cloud optical properties in the ECMWF model. *Mon. Wea. Rev.*, **118**, 847-873.

Smedman, A. S., Tjernström, M., and Högström, U. (1993). Analysis of the turbulencestructure of a marine low-level jet. *Bound.-Layer Meteor.*, **66**, 105-126.

Tjemkes, S.A., and Duynkerke, P.G. (1989). The nocturnal boundary layer: calculations compared with observations. *J. of Appl. Meteor.*, **28**, 161-175.

Van de Wiel, B. J. H, Ronda, R. J., Moene, A. F., De Bruin, H. A. R., and Holtslag, A. A. (2002). Intermittent Turbulence and Oscillations in the Stable Boundary Layer over Land. Part I: A Bulk Model. *J. Atmos. Sci.*, **59**, 942-958.

Wyngaard, J.C. and Brost, R.A. (1984). Top-Down and Bottom-Up diffusion of a scalar in the Convective Boundary Layer *J. Atmos. Sci.*, **41**, 102-112.